

Incremental Binding Free Energies in Mg²⁺ Complexes: A DFT Study

Todor Dudev^{†,§} and Carmay Lim^{*,†,‡}

Institute of Biomedical Sciences, Academia Sinica, Taipei 11529, Taiwan, R.O.C., and Department of Chemistry, National Tsing Hua University, Hsinchu 300, Taiwan, R.O.C.

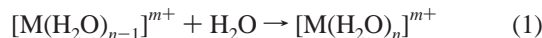
Received: May 14, 1999; In Final Form: August 10, 1999

Density functional theory has been employed to evaluate the incremental binding energies, enthalpies, entropies, and free energies for the reactions of Mg²⁺ with water, methanol, formamide, and formate. The B3LYP/6-31+G* calculations on the Mg²⁺ complexes show that the metal ion can accommodate no more than three negatively charged formates. For the neutral-ligand complexes, magnesium prefers to bind to methanol and formamide rather than water when the number of ligands is less than four, but it prefers water to methanol and formamide for complexes with five or six ligands. These results have been rationalized in terms of steric crowding of the ligands around the metal ion and charge transfer from the ligand(s) to Mg²⁺. These two factors result in attenuation of the Mg–O bond distance and, hence, reduction in the electrostatic and polarization energies, which dominate the incremental binding energy. An empirical scheme, employing the incremental binding energies for Mg²⁺–single-type-ligand complexes, has been developed to accurately predict the total binding energy of Mg²⁺–mixed-ligand clusters.

Introduction

In recent years, there has been growing interest in studying the mechanism of metal ion complexation with various ligands to elucidate the factors governing metal–ligand complexation and the role of metal ions in various chemical, photochemical, and biochemical processes.^{1–3} Gas-phase experiments on metal ion complexation provide an unique opportunity to study the process in detail, free from intermolecular interactions. The gas-phase studies provide a wealth of information on ion–ligand vs ion–solvent interactions. They also constitute a bridge between gas phase and solution. For example, the difference in the total hydration enthalpy or free energy between magnesium and calcium can be obtained from the differences in the first- and second-shell hydration enthalpy or free energy.⁴

Determination of gas-phase equilibria involving monocations were initiated by Kebarle and co-workers about 30 years ago.^{5,6} Singly charged ion clusters [M(H₂O)_n]⁺ were formed by spontaneous ion–solvent molecule association reactions. Incremental enthalpies, entropies, and free energies for the hydration reaction



were measured for aqua complexes of *monovalent* alkali metals: Li⁺, Na⁺, K⁺, Rb⁺, and Cs⁺. However, these thermodynamic parameters could not be measured for divalent alkaline earth metals since collisions of doubly charged ions M²⁺ possessing high second ionization energies with water molecules having low ionization energies result in M²⁺ + 2H₂O → [M(OH)]⁺ + H₃O⁺. Recent advances in techniques such as electrospray ionization^{4,7,8} and blackbody infrared radiative dissociation^{9,10} have produced doubly charged ion clusters [M(H₂O)_n]²⁺ by ion transfer from solution to the gas phase. Furthermore, equilibria (eq 1) involving Mg²⁺, Ca²⁺, Sr²⁺, and

Ba²⁺ have been determined at different temperatures to yield incremental enthalpies, entropies, and free energies. Although first- and second-hydration-shell binding energies are available for alkali metal monocations, only the outer-hydration-shell thermodynamic changes (*n* = 6–14 in eq 1) for alkaline earth dication have been measured^{7–10} since, for low *n*, eq 1 requires high temperatures (see below and Table 1), which are inaccessible with present experimental techniques.

On the other hand, for low (*n* – 1, *n*) equilibria (eq 1), quantum mechanical methods can be used to compute reliable binding energies.^{11–14} Since quantum mechanical calculations become computationally prohibitive for higher (*n* – 1, *n*) equilibria, they nicely complement the experimental data. For (*n* – 1, *n*) equilibria where theoretical and experimental energies are available, the two sets of data are in excellent agreement. Although the absolute numbers depend on the method and basis set used, there is a consensus in the literature that the first-shell incremental hydration enthalpies (−Δ*H*^{n–1,n}) depend on the number of bound water molecules. For example, MP2/6-31+G*/HF/6-31+G*¹¹ and B3LYP/6-311++G(2d,2p)//B3LYP/LANL2DZ¹² calculations show that the energy gain upon binding the first and sixth water to Mg²⁺ is 77–82 and 25–29 kcal/mol, respectively (see Table 1); for Ca²⁺, the range is 54–29 kcal/mol, for Sr²⁺, 48–27 kcal/mol, and for Ba²⁺, 41–24 kcal/mol.¹¹ Furthermore, when the incremental binding energy is less than 12–14 kcal/mol, “*n* + *m*” clusters in which *n* and *m* water molecules reside in the first and second hydration shell, respectively, were found to be more stable than clusters with all waters in the primary shell. However, the latter are more stable for small (*n* = 1–6) [M(H₂O)_n]²⁺ clusters with incremental binding energies greater than 14 kcal/mol.¹¹ In most cases the binding energies^{11,12,14} or enthalpies,¹¹ rather than free energies, have been evaluated. Thus, the role of entropy in the metal–ligand complex formation remains unclear. Furthermore, the complexation of alkaline earth metal dications with nonwater ligands of biological relevance has not been systematically explored.

Here density functional theory (DFT) calculations have been

[†] Academia Sinica.

[‡] National Tsing Hua University.

[§] On leave from the Department of Chemistry, University of Sofia, Bulgaria.

TABLE 1: Incremental binding enthalpies $\Delta\Delta H^{n-1,n}$ (in kcal/mol) at 298.15 K for $[\text{Mg}(\text{H}_2\text{O})_{n-1}]^{2+} + \text{H}_2\text{O} \rightarrow [\text{Mg}(\text{H}_2\text{O})_n]^{2+}$

<i>n</i>	B3LYP/ 6-31+G* ^a	MP2/6-31+G*// HF/6-31+G* ^{b,c}	B3LYP/6-311+G(2d,2p)// B3LYP/LANL2DZ ^c
1	-81.2	-77.4 (+4.7%)	-81.5 (0.4%) ^d
2	-70.4	-68.1 (+3.3%)	-70.9 (0.7%) ^d
3	-55.4	-55.9 (-0.9%)	-55.1 (0.5%) ^d
4	-44.1	-44.9 (-1.8%)	-43.9 (0.5%) ^d
5	-28.2	-29.4 (-4.3%)	-28.0 (0.7%) ^d
6	-25.4	-29.1 (-14.6%)	-25.9 (2.0%) ^e

^a Present work. ^b Taken from ref 11. ^c Numbers in parentheses are percentage difference relative to the numbers in column 2. ^d Taken from ref 12; values are incremental binding energies including zero-point energies obtained from Hartree-Fock frequencies scaled by 0.90. ^e Taken from ref 4.

carried out to evaluate the incremental binding energies and enthalpies, as well as incremental binding entropies and free energies for the reaction of Mg^{2+} with water, methanol, formamide, and formate. The latter three ligands are commonly used to model the serine side chain, the asparagine or glutamine side chain or backbone carbonyl group, and the aspartic or glutamic acid side chain. The DFT calculations and energy decomposition analyses are outlined in Methods. Structures having up to six ligands in the inner coordination shell are considered. The structures of the Mg^{2+} complexes and the incremental binding thermodynamic parameters upon successive ligand binding are presented in Results. An empirical scheme that accurately predicts the total binding energies of mixed-ligand Mg^{2+} complexes (i.e., Mg^{2+} bound to ligands of different types) is also presented in Results. The incremental binding energies are decomposed into individual components and the major factors governing the energy changes are identified in Discussion. The key findings of this work are highlighted in Conclusion.

Methods

DFT Calculations. The DFT calculations employed Becke's three parameter hybrid method¹⁵ in conjunction with the Lee, Yang, and Parr correlation functional.¹⁶ The 6-31+G* basis set was employed since it has been shown to yield structures and binding energies that are in reasonable agreement with those obtained at a higher level of theory.¹¹ It also represents a reasonable compromise between performance and computational expense.^{11,17} The geometries of the magnesium complexes, assuming the symmetries in Table 2, were optimized at the B3LYP/6-31+G* level using the Gaussian 94 program.¹⁸ Vibrational frequencies were computed to verify that each cluster was at the minimum of its potential energy surface. No structures having imaginary frequencies were found. The zero point energy (ZPE), thermal correction (E_{TRV}), and entropy (S_{TRV}) were evaluated with the frequencies scaled by an empirical factor of 0.9613¹⁹ using standard statistical mechanical formulas.²⁰ The enthalpy, ΔH^n , and free energy, ΔG^n , for each complexation reaction $M + nL \rightarrow [M(L)_n]$ were computed from the differences in ΔE_{elec} , ΔZPE , ΔE_{TRV} , and ΔS_{TRV} between the product and reactants at room temperature, $T = 298.15$ K, according to the following expressions:

$$\Delta H^n = \Delta E_{\text{elec}} + \Delta ZPE + \Delta E_{\text{TRV}} + n\Delta PV \quad (2a)$$

$$\Delta G^n = \Delta H^n - T\Delta S_{\text{TRV}} \quad (2b)$$

where n is the number of ligands in the complex. Incremental enthalpies ($X = H$), entropies ($X = S$), and free energies ($X =$

TABLE 2: Incremental Binding Energies, Enthalpies, Entropies, and Free Energies at 298.15 K for Mg^{2+} Complexed with Water, Methanol, Formamide, and Formate^a

<i>n</i>	symmetry	$\Delta\Delta E^{n-1,n}$ (kcal/mol)	$\Delta\Delta H^{n-1,n}$ (kcal/mol)	$T\Delta\Delta S^{n-1,n}$ (kcal/mol)	$\Delta\Delta G^{n-1,n}$ (kcal/mol)
$[\text{Mg}(\text{H}_2\text{O})_n]^{2+}$					
1	C_{2v}	-83.8	-81.2	-7.2	-74.0
2	D_{2d}	-74.4	-70.4	-8.5	-61.9
3	D_3	-59.8	-55.4	-9.6	-45.8
4	S_4	-48.1	-44.1	-8.8	-35.3
5	C_{2v}	-32.7	-28.2	-10.6	-17.6
6	T_h	-29.8	-25.4	-12.2	-13.2
$[\text{Mg}(\text{CH}_3\text{OH})_n]^{2+}$					
1	C_s	-96.4	-94.6	-7.2	-87.4
2	C_2	-81.4	-78.1	-9.2	-68.9
3	C_3	-61.7	-57.8	-10.4	-47.4
4	S_4	-47.1	-43.7	-9.8	-33.9
5	C_1	-28.4	-25.4	-11.9	-13.5
6	S_6	-25.9	-22.2	-12.4	-9.8
$[\text{Mg}(\text{HCONH}_2)_n]^{2+}$					
1	C_s	-127.1	-123.5	-8.1	-115.4
2	C_2	-102.0	-97.5	-9.7	-87.8
3	C_3	-69.0	-65.2	-10.6	-54.6
4	S_4	-48.7	-45.6	-10.3	-35.3
5	C_1	-27.6	-24.4	-12.3	-12.1
6	C_1	-24.0	-21.8	-10.9	-10.9
$[\text{Mg}(\text{HCOO})_n]^{2+}$					
1	C_{2v}	-366.9 (-342.4) ^b	-363.1	-8.5	-354.6
2	D_{2d}	-209.6 (-205.2) ^b	-205.1	-11.2	-193.9
3	D_3	-55.9 (-55.9) ^b	-53.2	-11.3	-41.9
4	S_4	+39.7 (+32.1) ^b	+28.7	-4.3	+33.0

^a Computed at the B3LYP/6-31+G* level (see Methods). ^b Numbers with and without parentheses correspond to the monodentate- and bidentate-bound formate, respectively.

G) were then evaluated as

$$\Delta\Delta X^{n-1,n} = \Delta X^n - \Delta X^{n-1} \quad (3)$$

Our previous study¹⁷ showed that including the basis set superposition error for Mg^{2+} complexes at the B3LYP/6-31+G* level of theory did not improve the accuracy of the results. Hence, this correction was not incorporated in the binding energies reported in this work.

Energy Decomposition Analysis. The binding energy of some complexes was decomposed into different fragments employing the reduced variational space (RVS) scheme of Stevens and Fink.²¹ The RVS analysis partitions the binding energy (ΔE) into electrostatic (ΔE_{S}), exchange (ΔE_{EX}), polarization (ΔE_{PL}), and charge transfer (ΔE_{CT}) contributions (see refs 21 and 22 for definitions of these components). The RVS energy decomposition analyses were carried out using the GAMESS program.²³ Calculations were performed at the HF/6-31+G*//B3LYP/6-31+G* level of theory since DFT methods have not been implemented in the GAMESS program. The HF/6-31+G* binding energies were slightly different from the respective B3LYP/6-31+G* energies, since the former excludes correlation, while the latter incorporates correlation via the exchange and correlation functional. Since direct mode is not available for the RVS analysis, hundreds of millions of two-electron integrals have to be stored on a hard disk for each run. Therefore, the RVS energy decomposition analyses were limited to magnesium clusters with three or fewer ligands.

Results

Calibration of Results. Experimental and previous theoretical results for the hydration of Mg^{2+} (see Introduction) can be used to assess the accuracy of the present calculations. For Mg^{2+} with $n = 6$ in eq 1, our computed $\Delta\Delta H^{5,6}$ (-25.4 kcal/mol)

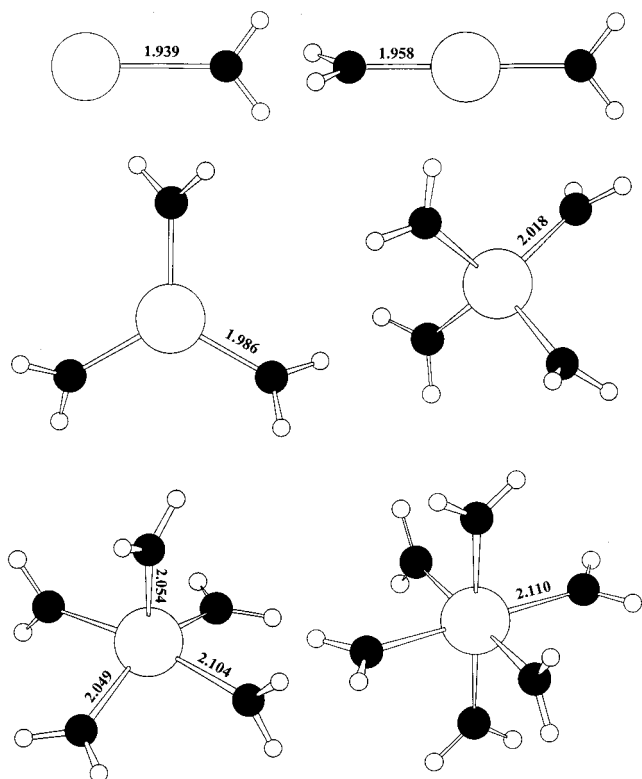


Figure 1. Ball and stick diagram of the lowest energy $[Mg(H_2O)_n]^{2+}$ ($n = 1, \dots, 6$) complexes.

agrees with the experimental number (-24.6 kcal/mol⁴) to within the experimental error of 1 kcal/mol. However, the computed $T\Delta\Delta S^{5,6}$ (-12.2 kcal/mol) is too negative compared to the experimental value (-8.7 ± 0.6 kcal/mol⁴) and hence, $\Delta\Delta G^{5,6}$ (-13.2 kcal/mol) is predicted to be too positive (by ~ 2 kcal/mol) compared to experiment (-16.0 ± 0.5 kcal/mol⁴). This suggests that incremental enthalpies can generally be predicted more accurately than the incremental entropies or free energies.

The structures and binding energies of the $[Mg(H_2O)_n]^{2+}$ complexes are in overall agreement with those obtained using a different method or a larger basis set. The Mg–O bond lengths in the B3LYP/6-31+G* optimized $[Mg(H_2O)_n]^{2+}$ complexes agree with the respective distances in the HF/6-31+G* and B3LYP/LANL2DZ optimized structures to within 0.004¹¹ and 0.03 Å,¹² respectively. The B3LYP/6-31+G* incremental binding enthalpies agree with the B3LYP/6-311++G(2d,2p)//B3LYP/LANL2DZ¹² incremental binding energies including zero-point energies to within 2% (see Table 1). Good agreement is also obtained between the B3LYP/6-31+G* and MP2/6-31+G*/HF/6-31+G* incremental binding enthalpies except for $\Delta\Delta H^{5,6}$ (Table 1). The MP2 calculations predict similar $\Delta\Delta H^{4,5}$ and $\Delta\Delta H^{5,6}$ values,¹¹ whereas the B3LYP calculations predict that $|\Delta\Delta H^{4,5}|$ is greater than $|\Delta\Delta H^{5,6}|$ by ~ 3 kcal/mol, even though the two sets of calculations predict a square-pyramidal (as opposed to a trigonal-bipyramidal) structure for $[Mg(H_2O)_5]^{2+}$ (see Figure 1).

Structures. Figures 1–4 show the fully optimized structures of the complexes with the lowest energy. Complexes with water, methanol, and formamide have similar ligand arrangement around the metal ion. However, the overall symmetry of the complexes containing methanol and formamide decreases since the symmetry of the nonaqua ligands is lower than that of water (see Table 2). In the complexes containing neutral ligands, the Mg–O distance lengthens with increasing ligand coordination.

The net change in the Mg–O distance from mono- to hexacoordinated magnesium, 0.17, 0.21, and 0.28 Å for the water, methanol, and formamide complexes, respectively, correlates with the increasing bulkiness of the ligand.

In contrast to the neutral-ligand Mg^{2+} complexes, the Mg–O distance in the $[Mg(HCOO)]^{2-n}$ complexes lengthens significantly (by ~ 0.2 Å) in going from mono- to tricoordinate magnesium, but decreases by almost an equal amount (0.18 Å) upon addition of a fourth formate. This is probably related to the change in the mode of formate binding to magnesium when more than three formates become bound to the metal. When the number of bound ligands is ≤ 3 , the formates prefer to bind in a bidentate fashion, occupying two, four, or six magnesium binding positions, but they prefer to bind in a monodentate fashion when four or more formates become bound to Mg^{2+} (see Figure 4). Note that strong electron correlation effects can be expected in the negatively charged $[Mg(HCOO)_3]^-$ and $[Mg(HCOO)_4]^{2-}$ complexes. While DFT incorporates correlation effects, it may not be adequate for handling negative species, and differential effects of correlation may also be important in these structures. However, in interpreting the results below, emphasis is placed on the trends in the changes of the incremental binding energies rather than their absolute values.

Incremental Enthalpies, Entropies, and Free Energies. Sequential binding energies ($\Delta\Delta E^{n-1,n}$), enthalpies ($\Delta\Delta H^{n-1,n}$), entropies ($T\Delta\Delta S^{n-1,n}$), and free energies ($\Delta\Delta G^{n-1,n}$) for magnesium complexed with water, methanol, formamide, and formate are tabulated in Table 2 and shown graphically as a function of n , the number of ligands bound to magnesium, in Figure 5. Incremental binding energies were also evaluated for Mg^{2+} –formate complexes ($n = 1–4$) with the formates monodentately bound. For these monodentate-formate complexes the Mg–O–C bond angles were fixed at 120° during the geometry optimization.

Complexes Containing Neutral Ligands (H_2O , CH_3OH , and $HCONH_2$). These complexes show similar trends in the incremental enthalpies, entropies, and free energies with increasing number of bound ligands (n). The magnitude of the incremental enthalpy and free energy gradually decreases with increasing n ; i.e., each successive addition of a neutral ligand results in a smaller gain in the binding enthalpy or free energy (Figure 5). This is due partly to the increasing repulsive interactions among the ligands as the complex becomes bulkier, resulting in longer Mg–O distances (see above and Figures 1–3) and thus weaker metal–ligand interactions. Unlike the incremental enthalpies and free energies, the $T\Delta\Delta S^{n-1,n}$ term shows a local minimum at $n = 3$ and a local maximum at $n = 4$ (see Figure 5c). This suggests a looser ligand packing for $[Mg(L)_4]^{2+}$ complexes relative to the $[Mg(L)_3]^{2+}$ clusters. The data summarized in Table 2 demonstrate the interplay between enthalpy and entropy in determining $\Delta\Delta G^{n-1,n}$. For the first four clusters in each series the enthalpy gain upon successive ligand coordination to Mg^{2+} contributes mainly to the free energy gain. However, for the penta- and hexacoordinated complexes the $T\Delta\Delta S^{n-1,n}$ term, which is roughly half $\Delta\Delta H^{n-1,n}$, also contributes to the incremental free energy. This trend is supported by the experimental observations of Kebarle and co-workers, who detected a significant entropic contribution to the gas-phase formation free energy of $[Mg(H_2O)_n]^{2+}$ ($n = 6–14$) clusters:⁴ the incremental free energies ranged from $\Delta\Delta G^{6,7} = -12.8$ to $\Delta\Delta G^{13,14} = -5.1$ kcal/mol, whereas $T\Delta\Delta S^{n-1,n}$ ($n = 7–14$) varied much less, between -7.6 and -6.6 kcal/mol.

Magnesium binding to one, two, or three water molecules is thermodynamically less favorable than complexation with the

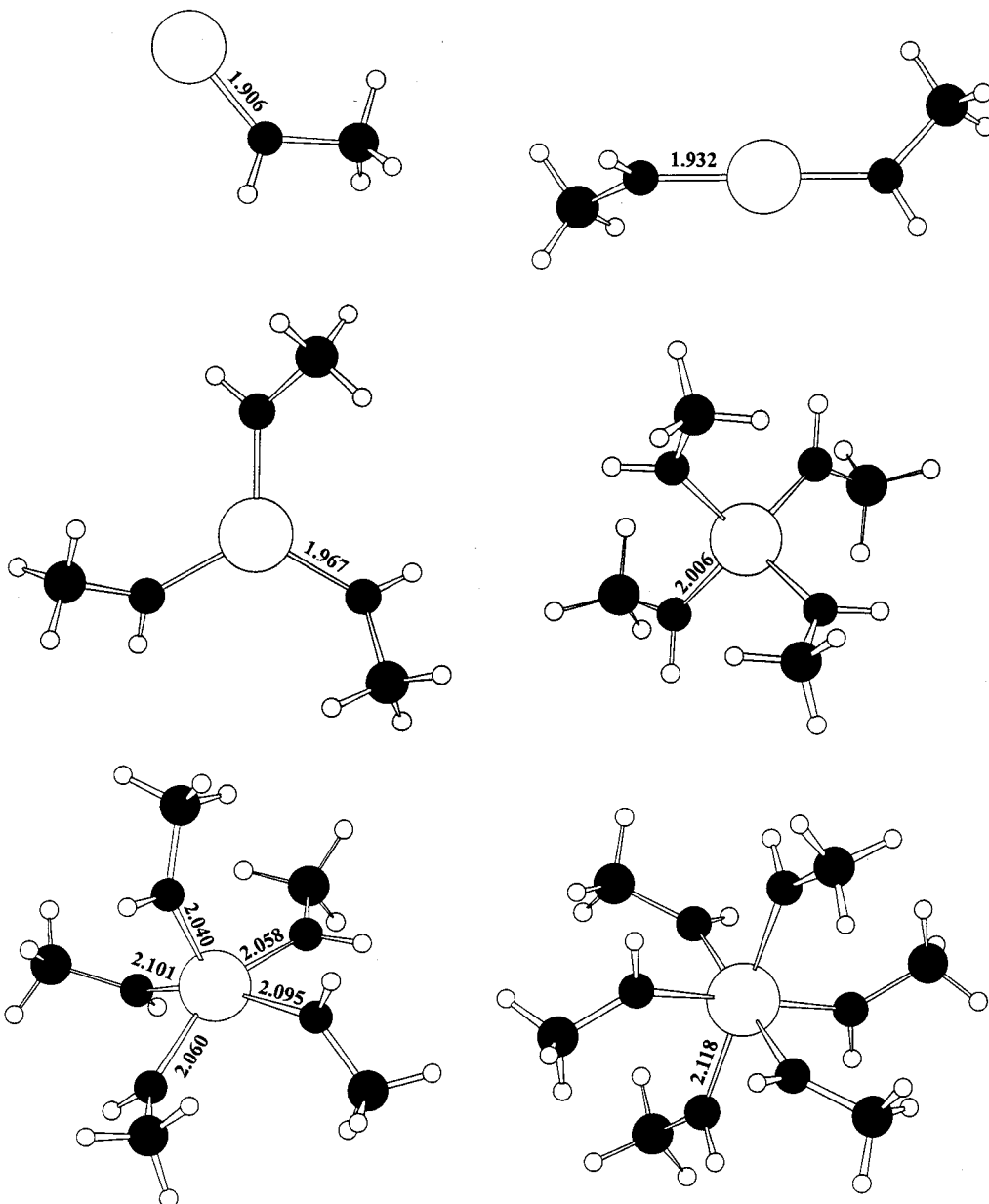


Figure 2. Ball and stick diagram of the lowest energy $[\text{Mg}(\text{CH}_3\text{OH})_n]^{2+}$ ($n = 1, \dots, 6$) complexes.

same number of methanol or formamide ligands. This is evident from the incremental free energies for Mg^{2+} complexes with three or fewer bound water molecules, which are lower in magnitude than those for the corresponding nonaqua complexes (Table 2). For example, the free energy gain upon reaction of Mg^{2+} with a water molecule is -74 kcal/mol, which is significantly lower than that with methanol (-87 kcal/mol) and formamide (-115 kcal/mol). Furthermore, as the number of bound ligands *increases*, the magnitude of $\Delta\Delta G^{n-1,n}$ for methanol and formamide complexes decreases more rapidly than that for the aqua complexes. Consequently, the $\Delta\Delta G^{3,4}$ values for Mg^{2+} complexed with water, methanol, or formamide are similar (about -35 kcal/mol), while for the tetra- and penta-coordinated clusters, coordination to another water molecule becomes thermodynamically more favored than complexation with another methanol or formamide (Table 2). The sequential binding energies and enthalpies follow the same trend of changes as the incremental free energies (Table 2 and Figure 5). Similar findings have been reported by Kebarle et al.,⁴ who compared $\Delta\Delta H^{n-1,n}$ for Mg^{2+} complexes with water and acetone. The

preliminary results for acetone complexes showed that the interactions with acetone at low n ($n = 1, 2, 3$) are stronger than those with water, but they attenuate sharply as n is increased so that the $\Delta\Delta H^{5,6}$ and $\Delta\Delta H^{6,7}$ values for acetone become lower than the corresponding ones for water.⁴

Complexes with Formate $[\text{Mg}(\text{HCOO})_n]^{2-n}$. Due to the strong charge–charge interactions, the trends in $\Delta\Delta H^{n-1,n}$ $T\Delta\Delta S^{n-1,n}$, and $\Delta\Delta G^{n-1,n}$ with increasing n for $[\text{Mg}(\text{HCOO})_n]^{2-n}$ complexes differ from those for the neutral-ligand clusters. The incremental enthalpies and free energies for the formate complexes become less favorable much more quickly with increasing n than those for the neutral-ligand complexes (Figure 5). The $T\Delta\Delta S^{n-1,n}$, $n \leq 3$, values for the formate complexes are more negative than the respective values for the water, methanol, and formamide clusters (Table 2, Figure 5c) due to the tight bidentate binding of the formates compared to the monodentate binding of the neutral ligands. In contrast, the $T\Delta\Delta S^{3,4}$ value is least negative for the complex containing negatively charged (as opposed to neutral) ligands (Table 2). This is related to the transition from the tightly structured $[\text{Mg}(\text{HCOO})_3]^-$ with bidentate-bound

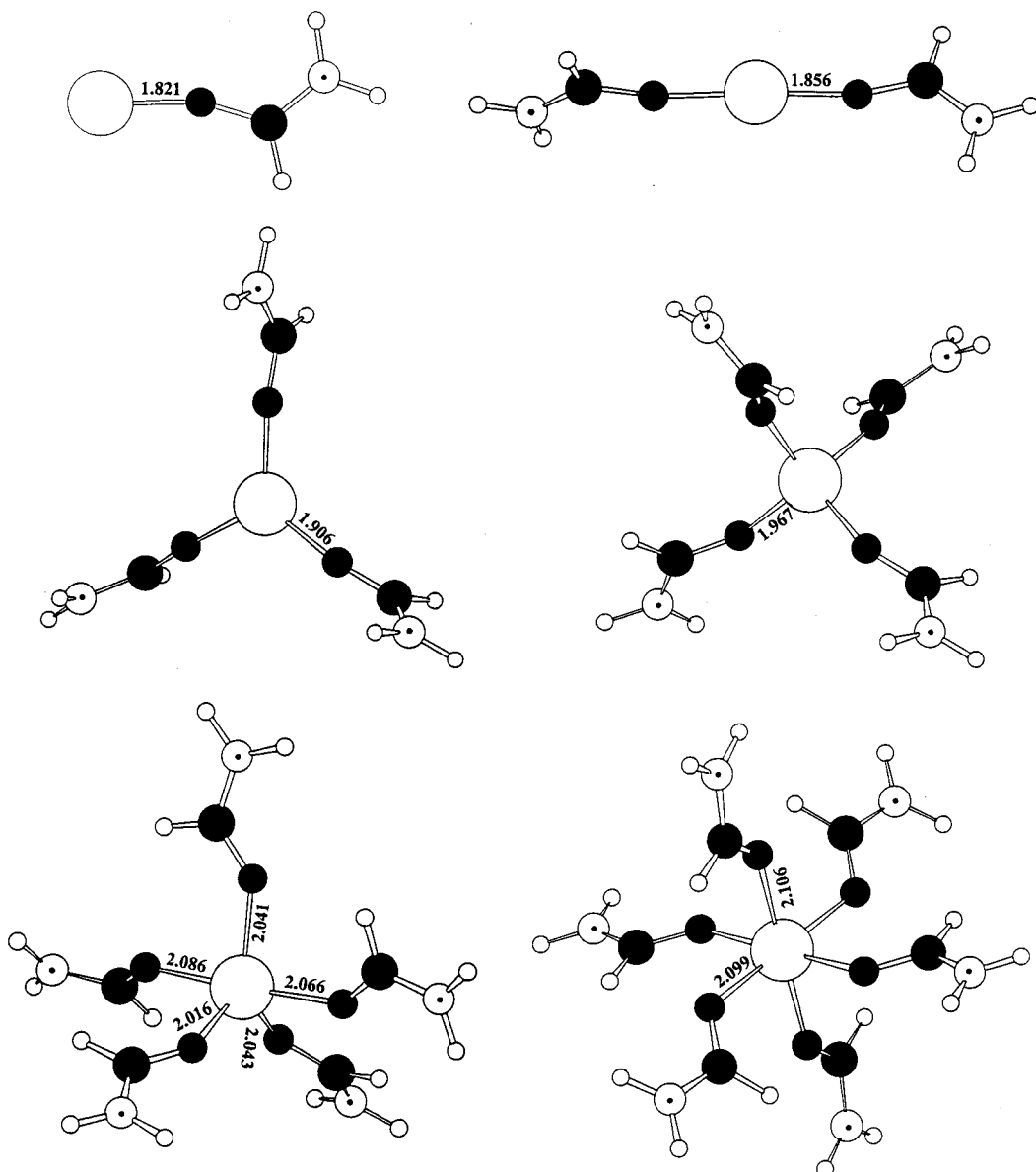


Figure 3. Ball and stick diagram of the $[Mg(HCONH_2)_n]^{2+}$ ($n = 1, \dots, 6$) complexes.

ligands occupying the six Mg^{2+} binding sites, to the much looser tetracoordinated complex with monodentate-bound ligands (see Figure 4).

The incremental free energy for the formate clusters is dominated by the enthalpy term. The binding of the first and second formate ligands to magnesium yields relatively large incremental enthalpies (-363 and -205 kcal/mol) and free energies (-355 and -194 kcal/mol) due to the strong electrostatic attraction between the oppositely charged ions. Binding of a third formate is still thermodynamically favorable even though the free energy gain is significantly reduced ($\Delta\Delta G^{2,3} = -42$ kcal/mol). However, the addition of a fourth $HCOO^-$ to the negatively charged $[Mg(HCOO)_3]^-$ complex is an unlikely process: the sequential free energy becomes positive ($\Delta\Delta G^{3,4} = +33$ kcal/mol). Binding of a fifth or sixth formate ligand is expected to be also unfavorable, and therefore, the respective structures were not examined in this study.

RVS Decomposition Analysis. Table 3 lists the electrostatic, polarization, and charge-transfer contributions to the incremental binding energies $\Delta\Delta E^{n-1,n}$. In Table 3, the electrostatic $\Delta\Delta ES^{n-1,n}$ and exchange repulsion $\Delta\Delta EX^{n-1,n}$ terms have been combined into the $\Delta\Delta ESX^{n-1,n}$ term, while the $\Delta\Delta PL_{Mg}$ (polarization of

Mg^{2+} by its ligands) and $\Delta\Delta CT_{Mg-L}$ (charge transfer from Mg^{2+} to its ligands) terms have been omitted since they contribute less than 0.1% to the overall incremental binding energy. Table 3 shows that the $\Delta\Delta ESX^{n-1,n}$ term and, to a lesser extent, the $\Delta\Delta PL_L^{n-1,n}$ term govern the incremental binding energy, while charge transfer from the ligand(s) to the metal ion contributes less than 4% to $\Delta\Delta E^{n-1,n}$. Note that the 6-31+G* basis set is known to underestimate the polarizability of water;¹¹ thus the magnitude of $\Delta\Delta PL_L^{n-1,n}$ and its percentage contribution to $\Delta\Delta E^{n-1,n}$ may be underestimated in Table 3. Thus, changes in the individual components as a function of n for a fixed ligand type or as a function of ligand type for fixed n are emphasized in the analysis below.

In a given ligand series, $\Delta\Delta ESX^{n-1,n}$, $\Delta\Delta PL_L^{n-1,n}$, $\Delta\Delta CT_{L-Mg}^{n-1,n}$, and hence $\Delta\Delta E^{n-1,n}$ decrease in absolute value in going from mono- to tri-ligand complexes. On the other hand, the percentage contributions of $\Delta\Delta PL_L$ and $\Delta\Delta CT_{L-Mg}$ to $\Delta\Delta E^{n-1,n}$ decrease with increasing n , while that of $\Delta\Delta ESX$ increases, suggesting that polarization and charge-transfer effects play a lesser role in stabilizing the heavier ($n > 3$) complexes where the $Mg-O$ distances are longer. In fact, the $\Delta\Delta PL^{2,3}$ and $\Delta\Delta CT_{L-Mg}^{2,3}$ terms for the formate complexes are positive.

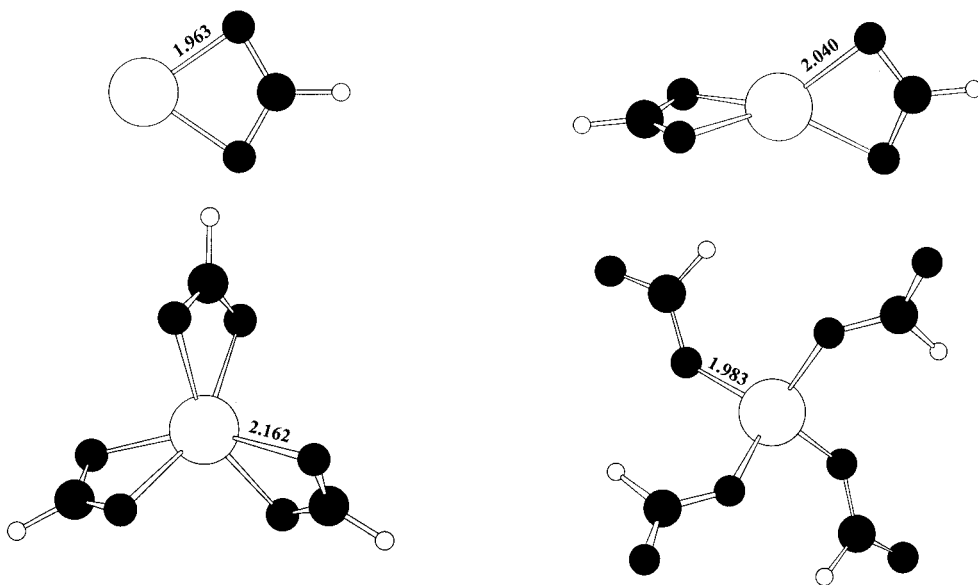


Figure 4. Ball and stick diagram of the lowest energy $[\text{Mg}(\text{HCOO}^-)_n]^{2-n}$ ($n = 1, \dots, 4$) complexes.

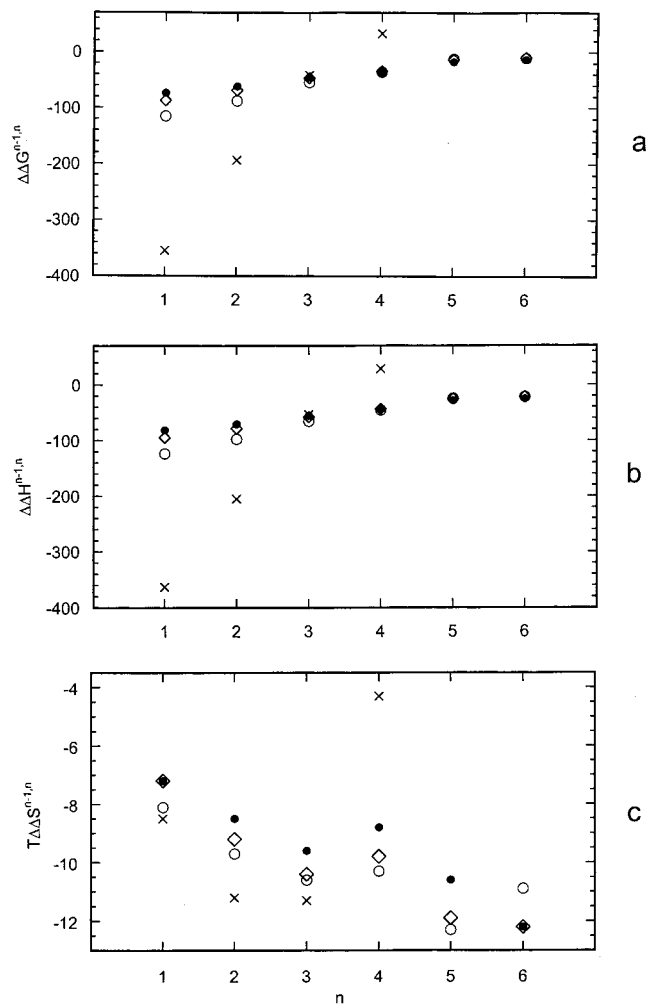


Figure 5. Incremental free energies $\Delta\Delta G^{n-1,n}$ (a), enthalpies $\Delta\Delta H^{n-1,n}$ (b), and entropies $T\Delta\Delta S^{n-1,n}$ (c) as a function of n , the number of ligands bound to magnesium. The filled circles, diamonds, open circles, and cross symbols represent the data points for the water, methanol, formamide, and formate complexes, respectively.

The magnitude of $\Delta\Delta ESX^{n-1,n}$ is determined by charge-charge and charge-dipole interactions for Mg^{2+} complexed with negatively charged and neutral ligands, respectively. Thus, for

TABLE 3: RVS Decomposition Analysis for Mg^{2+} Complexed with Water, Methanol, Formamide, and Formate^a

n	$\Delta\Delta ESX^{n-1,n}$ (kcal/mol)	$\Delta\Delta PL_L^{n-1,n}$ (kcal/mol)	$\Delta\Delta CT_{L-\text{Mg}}^{n-1,n}$ (kcal/mol)	$q_{\text{Mg}}^{\text{CHELG}}$ (e)
	$[\text{Mg}(\text{H}_2\text{O})_n]^{2+}$			
1	-53.2 (66%)	-25.0 (30%)	-2.9 (3.6%)	1.93
2	-51.8 (69%)	-20.8 (28%)	-1.9 (2.6%)	1.82
3	-48.8 (78%)	-13.6 (21%)	-0.3 (0.3%)	1.77
	$[\text{Mg}(\text{CH}_3\text{OH})_n]^{2+}$			
1	-57.6 (58%)	-38.0 (38%)	-3.4 (3.4%)	1.87
2	-54.2 (63%)	-29.6 (34%)	-2.6 (2.6%)	1.57
3	-49.1 (73%)	-18.2 (26%)	-0.7 (1.0%)	1.37
	$[\text{Mg}(\text{HCONH}_2)_n]^{2+}$			
1	-75.4 (56%)	-54.4 (41%)	-4.0 (3.0%)	1.85
2	-69.7 (62%)	-40.0 (35%)	-2.6 (2.3%)	1.48
3	-59.7 (76%)	-19.0 (23%)	-0.9 (1.0%)	1.21
	$[\text{Mg}(\text{HCOO})_n]^{2-n}$			
1	-303.2 (82%)	-52.3 (14%)	-12.6 (3.4%)	1.58
2	-205.8 (93%)	-14.1 (6%)	-3.2 (1.3%)	1.34
3	-73.4 (128%)	+14.8 (-26%)	+1.1 (-2.0%)	1.63

^a Results were obtained at the HF/6-31+G*/B3LYP/6-31+G* level (see Methods). Note that the $\Delta\Delta E^{n-1,n}$ energies obtained from the sums of the energy components in the table differ from the $\Delta\Delta E^{n-1,n}$ values in Table 2 because the latter include correlation while the former does not (see Methods).

at a given n , the magnitude of $\Delta\Delta ESX^{n-1,n}$ in the $[\text{Mg}(\text{HCOO})_n]^{2-n}$ cluster is larger than the respective value in complexes with water, methanol, and formamide, and increases in the order, $\text{H}_2\text{O} \approx \text{CH}_3\text{OH} < \text{HCONH}_2 < \text{HCOO}^-$. The magnitude of the $\Delta\Delta PL_L^{n-1,n}$ polarization term correlates with the mean polarizability of the neutral ligands ($\overline{\alpha}_{\text{H}_2\text{O}} = 6.9 \text{ au}^3$, $\overline{\alpha}_{\text{CH}_3\text{OH}} = 18.0 \text{ au}^3$; and $\overline{\alpha}_{\text{HCONH}_2} = 25.0 \text{ au}^3$), and increases as $\text{H}_2\text{O} < \text{CH}_3\text{OH} < \text{HCONH}_2$. As expected, for a cluster of given n , the magnitude of the charge-transfer energy is anticorrelated with the (ChelpG)²⁴ charge on magnesium, which, in turn, is anticorrelated with the Mg–O distance. For example, among the monocoordinated ($n = 1$) complexes, formation of $[\text{Mg}(\text{HCOO})]^{+}$ results in the most favorable $\Delta\Delta CT_{\text{L-Mg}}^{0,1}$ (-12.6 kcal/mol) and, thus, the least electropositive magnesium (1.58) and longest Mg–O distance (1.963 Å). Among the neutral ligands, formamide appears to be the strongest electron-donating ligand and water the poorest.

It should be noted that although the charge-transfer terms do not contribute significantly to the incremental binding energy, charge transfer does *indirectly* affect the energetics of the complex formation. The partial neutralization of the positive charge on magnesium caused by charge transfer results in longer Mg—O distances and, thus, smaller $|\Delta\Delta\text{ESX}^{n-1,n}|$ and $|\Delta\Delta\text{PL}_L^{n-1,n}|$ values, which depend on the magnitude of the charge and the Mg—O distance. The role of charge transfer in forming the metal-ligand complexes has also been emphasized by other authors.^{4,12}

Total Binding Energy of Mixed-Ligand Magnesium Complexes. Incremental binding energies $\Delta\Delta E^{n-1,n}$ calculated for the single-type-ligand complexes can be used to estimate the total binding energies ΔE_{total} in mixed-ligand Mg²⁺ complexes. Calculations on smaller-size ($n = 2-4$) mixed-ligand magnesium complexes (data not shown) show that the ΔE_{total} is *not* an additive sum of the incremental binding energies evaluated for the single-type-ligand Mg²⁺ complexes. The sequential energies for a given ligand depends strongly on the type of ligand already bound to the magnesium cation. For example, the incremental binding energy $\Delta\Delta E^{1,2}$ for water decreases in magnitude by 4% in [Mg(H₂O)(CH₃OH)]²⁺, by 8% in [Mg(H₂O)(HCONH₂)]²⁺, by 30% in [Mg(H₂O)(HCOO)]⁺, and by 40% in [Mg(H₂O)(HCOO)₂]⁰. These percentage variations correlate with the amount of positive charge reduction on the magnesium by charge transfer from the nonaqua ligand(s) (see Table 3). The percentage drop in the magnitude of $\Delta\Delta E^{1,2}$ for the other nonaqua ligands were also obtained.

Taking into account these interdependencies, the total binding energy of the mixed-ligand magnesium complexes can be approximated by the following empirical expressions assuming that formates (f) bind first to Mg²⁺, followed by formamide (a), methanol (m), and water (w). For complexes with *one* formate

$$\Delta E_{\text{total}} = \Delta\Delta E_f^{0,1} + 0.74 \sum_{i=2}^{N+1} \Delta\Delta E_a^{i-1,i} + 0.70 \left(\sum_{j=N+2}^{N+M+1} \Delta\Delta E_m^{j-1,j} + \sum_{k=N+M+2}^{N+M+Q+1} \Delta\Delta E_w^{k-1,k} \right) \quad (4)$$

In eq 4, N is the total number of formamides in the complex, M the number of methanols, and Q the number of waters. For complexes with *two and three* formates

$$\Delta E_{\text{total}} = \sum_{i=1}^P \Delta\Delta E_f^{i-1,i} + c_2 \left(\sum_{j=P+1}^{P+N} \Delta\Delta E_a^{j-1,j} + \sum_{k=P+N+1}^{P+N+M} \Delta\Delta E_m^{k-1,k} + \sum_{l=P+N+M+1}^{P+N+M+Q} \Delta\Delta E_w^{l-1,l} \right) \quad (5)$$

where P is the total number of formates in the complex; $c_2 = 0.55$ for diformate complexes and $c_3 = 0.45$ for triformalate complexes, respectively. For complexes with *formamide, methanol, and water*

$$\Delta E_{\text{total}} = \sum_{i=1}^N \Delta\Delta E_a^{i-1,i} + (1.0 - 0.1N) \sum_{j=N+1}^{N+M} \Delta\Delta E_m^{j-1,j} + (1.0 - 0.05M)(1.0 - 0.1N) \sum_{k=M+N+1}^{N+M+Q} \Delta\Delta E_w^{k-1,k} \quad (6)$$

For complexes with *formamide and water*

$$\Delta E_{\text{total}} = \sum_{i=1}^N \Delta\Delta E_a^{i-1,i} + (1.0 - 0.1N) \sum_{j=N+1}^{N+Q} \Delta\Delta E_w^{j-1,j} \quad (7)$$

For complexes with *methanol and water*

$$\Delta E_{\text{total}} = \sum_{i=1}^M \Delta\Delta E_m^{i-1,i} + (1.0 - 0.05M) \sum_{j=M+1}^{M+Q} \Delta\Delta E_w^{j-1,j} \quad (8)$$

The $\Delta\Delta E^{n-1,n}$ values in Table 2 were used in eqs 4–8 to evaluate the total binding energy in various hexacoordinated mixed-ligand Mg²⁺ complexes. To verify the predicted energies, the corresponding ΔE_{total} values were obtained for the same complexes after B3LYP/6-31+G* geometry optimization. Table 4 shows that the “empirical” and the ab initio ΔE_{total} are in close agreement; in most cases the “empirical” binding energies are within 1% of the respective ab initio values. Consequently, ΔE_{total} of another 40 magnesium complexes containing different numbers of water, methanol, formamide, and formate ligands were evaluated using eqs 4–8 (see Table 5). Note that ab initio geometry optimization of some of the heavier complexes containing more than 350 basis functions took 3–4 weeks of CPU time on a HP 9000 workstation. Thus, the proposed analytical formulas provide a rapid way to estimate the binding energies in a large spectrum of Mg²⁺ complexes. Such an approach may also be applied to experimentally evaluated $\Delta\Delta E^{n-1,n}$, provided that the full set of experimental sequential energies in single-type-ligand complexes is available.

Discussion

Two factors determine the incremental binding energies in magnesium complexes: (i) steric crowding of the ligand(s) around the metal ion and (ii) charge transfer from the ligand to the magnesium dication. As the number of coordinated ligands increases, the steric repulsion among them leads to lengthening of the Mg—O bond distance, which, in turn, results in a lowering of the $\Delta\Delta\text{ESX}^{n-1,n}$ and $\Delta\Delta\text{PL}_L^{n-1,n}$ energies and hence $\Delta\Delta E^{n-1,n}$. On the other hand, charge transfer from the ligand(s) reduces the positive charge on the metal ion (Table 3). As the number of bound neutral ligands increases, the positive charge on magnesium decreases. The most pronounced charge reduction occurs in the mono- and biformate complexes, where the net charge on magnesium drops to 1.58e and 1.34e, respectively (see Table 3 and Results). The partial neutralization of the charge on the metal ion leads to weakening of the metal-ligand interactions (longer Mg—O distance), and thus to lowering of the electrostatic and polarization energies (Table 3).

These two factors help to explain the observed changes in $\Delta\Delta H^{n-1,n}$ and $\Delta\Delta G^{n-1,n}$ upon successive addition of water, methanol, and formamide to Mg²⁺ (Table 2, Figure 5). The free energy gain upon binding the first three nonaqua ligands successively to Mg²⁺ is greater than the respective gain upon hydration; i.e., Mg²⁺ prefers to coordinate with methanol and formamide than with water for small ($n \leq 3$) complexes. This is mainly due to the stronger charge-dipole (ΔESX) and/or charge-induced dipole (ΔPL_L) interactions for methanol and formamide relative to those for water in these small ($n \leq 3$) complexes (see Table 3), as evidenced by the shorter Mg—O distance in [Mg(HCONH₂)_n]²⁺ and [Mg(CH₃OH)_n]²⁺ compared to the respective distance in the hydrated complex for a given n ($n \leq 3$). However, as the first coordination shell of magnesium becomes completed ($n > 4$), the free energy gain upon hydration becomes greater than the respective gain accompanying complexation with the nonaqua ligands. This is due to the fact that

TABLE 4: Comparison Between ab Initio and Empirical ΔE_{total} for Mg^{2+} Mixed-Ligand Complexes

ligands ^a	$-\Delta E_{\text{total,DFT}}^b$ (kcal/mol)	$-\Delta E_{\text{total,emp}}^c$ (kcal/mol)	% deviation ^d
5w+1f	524.6	513.8	-2.0
4w+1a+1f	531.8	537.2	+1.0
3w+2a+1f	539.8	546.3	+1.2
2w+3a+1f	548.4	548.8	+0.1
1w+4a+1f	551.6	546.3	-1.0
5a+1f	549.1	543.2	-1.1
3w+1a+2f	643.8	646.4	+0.4
2w+2a+2f	642.5	646.7	+0.6
1w+3a+2f	640.8	643.9	+0.5
2w+1a+3f	668.5	668.8	0.04
5w+1a	343.9	347.4	+1.0
4w+2a	357.1	365.4	+2.3
3w+3a	369.8	375.5	+1.5
2w+4a	379.4	384.3	+1.3
1w+5a	390.2	389.3	-0.2
5w+1m	330.9	329.0	-0.6
4w+2m	333.1	331.2	-0.6
3w+3m	335.2	333.5	-0.5
2w+4m	337.1	336.6	-0.1
1w+5m	339.1	337.4	-0.5

^a Abbreviations: w, water; f, formate; a, formamide; m, methanol.

^b From B3LYP/6-31+G* ab initio calculations. ^c Using eqs 4–8 and incremental binding energies in Table 2. ^d Percentage deviations of the predicted values from ab initio calculated energies.

TABLE 5: Predicted ΔE_{total} (in kcal/mol) for Mg^{2+} Complexes

ligands ^a	$-\Delta E_{\text{total}}$	ligands ^a	$-\Delta E_{\text{total}}$
4a+2f	640.7	1w+1a	194.1
1w+2a+3f	666.5	2w+1a	247.9
3a+3f	663.9	3w+1a	291.2
1a+4w+1m	346.0	4w+1a	320.6
1a+3w+2m	345.5	1w+2a	276.9
1a+2w+3m	346.1	2w+2a	315.4
1a+1w+4m	345.3	3w+2a	341.6
1a+0w+5m	347.1	1w+3a	331.8
1f+4w+1m	518.7	2w+3a	354.7
1f+3w+2m	520.0	1w+4a	366.4
1f+2w+3m	519.3	1w+1m	167.1
1f+1w+4m	516.3	2w+1m	223.9
1f+0w+5m	513.5	3w+1m	269.6
2f+3w+1m	642.4	4w+1m	300.6
2f+2w+2m	641.8	1w+2m	231.6
2f+1w+3m	639.4	2w+2m	274.9
2f+0w+4m	637.2	3w+2m	304.3
3f+2w+1m	668.1	1w+3m	280.4
3f+1w+2m	666.2	2w+3m	308.2
3f+0w+3m	664.4	1w+4m	312.8

^a Abbreviations: w, water; f, formate; a, formamide; m, methanol.

water is a smaller ligand and a poorer electron donor compared to methanol and formamide. The Mg–O distance, which reflects steric repulsion among the ligands and the strength of the metal–ligand interactions, increases by 0.17 Å in going from the mono- to hexahydrate complex, but it increases even more, by 0.21 and 0.28 Å for the methanol and formamide complexes, respectively. Moreover, since water is a poorer electron donor compared to methanol and formamide, magnesium charge neutralization in water complexes is less than that in the respective methanol and formamide complexes (Table 3).

Conclusions

The B3LYP/6-31+G* calculations on Mg^{2+} complexed with water, methanol, formamide, and formate show that the metal ion can accommodate no more than three negatively charged formates (see Table 2 and Figure 5). In the case of Mg^{2+}

complexed with neutral ligands, binding to methanol and formamide is more favorable than that to water when the number of ligands is less than four. However, for complexes with five or six ligands, water appears to be favored over methanol and formamide in completing the first coordination shell. Two factors can largely account for the present findings: (1) steric crowding of the ligands around the metal ion and (2) charge transfer from the ligand(s) to Mg^{2+} . These two factors result in attenuation of the Mg–O bond distance, which, in turn, causes a reduction in $\Delta\Delta\text{ESX}_{n-1,n}$ and $\Delta\Delta\text{PL}_{L,n-1,n}$ energies, and hence $\Delta\Delta E_{n-1,n}$. An empirical scheme, employing the incremental binding energies $\Delta\Delta E_{n-1,n}$ for Mg^{2+} –single-type-ligand complexes, has been proposed to predict the total binding energy of Mg^{2+} –mixed-ligand clusters. The empirical formulas have been validated by reproducing the DFT binding energies of Mg^{2+} complexed with various ligand types.

Acknowledgment. T.D. is supported by the Institute of Biomedical Sciences. C.L. is supported by the Institute of Biomedical Sciences at Academia Sinica, the National Center for High Performance Computing, and the National Science Council, Republic of China (NSC-88-2113-M-001).

References and Notes

- Williams, A. F.; Floriani, C.; Merbach, A. E., Eds.; *Perspectives in Coordination Chemistry*; VCHA: Basel, 1992.
- Burgess, J. *Ions in Solution: Basic Principles of Chemical Interactions*; Ellis Horwood Ltd.: Chichester, England, 1988.
- Richens, D. T. *The Chemistry of Aqua Ions*; Wiley: Chichester, England, 1997.
- Peschke, M.; Blades, A. T.; Kebarle, P. *J. Phys. Chem. A* **1998**, *102*, 9978.
- Searles, S. K.; Kebarle, P. *J. Phys. Chem.* **1968**, *72*, 742.
- Dzidic, I.; Kebarle, P. *J. Phys. Chem.* **1970**, *74*, 1966.
- Blades, A. T.; Jayaweera, P.; Ikonomou, M. G.; Kebarle, P. *J. Chem. Phys.* **1990**, *92*, 5900.
- Blades, A. T.; Jayaweera, P.; Ikonomou, M. G.; Kebarle, P. *Int. J. Mass Spectrom. Ion Processes* **1990**, *101*, 325; **1990**, *102*, 251.
- Rodríguez-Cruz, S. E.; Jockusch, A.; Williams, E. R. *J. Am. Chem. Soc.* **1998**, *120*, 5842.
- Rodríguez-Cruz, S. E.; Jockusch, A.; Williams, E. R. *J. Am. Chem. Soc.* **1999**, *121*, 1986.
- Glendening, E. D.; Feller, D. *J. Phys. Chem.* **1996**, *100*, 4790.
- Pavlov, M.; Siegbahn, P. E. M.; Sandström, M. *J. Phys. Chem. A* **1998**, *102*, 219.
- Markham, G. D.; Glusker, J. P.; Bock, C. L.; Trachtman, M.; Bock, C. W. *J. Phys. Chem.* **1996**, *100*, 3488.
- Klobukowski, M. *Can. J. Chem.* **1992**, *70*, 589.
- Becke, A. D. *J. Chem. Phys.* **1993**, *98*, 5648.
- Lee, C.; Yang, W.; Parr, R. G. *Phys. Rev.* **1988**, *B37*, 785.
- Dudev, T.; Lim, C. *J. Am. Chem. Soc.* **1999**, *121*, 7665.
- Frisch, M. J.; Trucks, G. W.; Schlegel, H. B.; Gill, P. M. W.; Johnson, B. G.; Robb, M. A.; Cheeseman, J. R.; Keith, T.; Petersson, G. A.; Montgomery, J. A.; Raghavachari, K.; Al-Laham, A.; Zakrzewski, V. G.; Ortiz, J. V.; Foresman, J. B.; Cioslowski, J.; Stefanov, B. B.; Nanayakkara, A.; Challacombe, M.; Peng, C. Y.; Ayala, P. Y.; Chen, W.; Wong, M. W.; Andres, J. L.; Replogle, E. S.; Gomperts, R.; Martin, R. L.; Fox, D. J.; Binkley, J. S.; Defrees, D. J.; Baker, J.; Stewart, J. P.; Head-Gordon, M.; Gonzalez, C.; Pople, J. A. *Gaussian 94*, Revision D.4; Gaussian, Inc.: Pittsburgh, PA, 1994.
- Wong, M. W. *Chem. Phys. Lett.* **1996**, *256*, 391.
- McQuarrie, D. A. *Statistical Mechanics*; Harper and Row: New York, 1976.
- Stevens, W. J.; Fink, W. H. *Chem. Phys. Lett.* **1987**, *139*, 15.
- Chen, W.; Gordon, M. S. *J. Phys. Chem.* **1996**, *100*, 14316.
- Schmidt, M. W.; Baldridge, K. K.; Boatz, J. A.; Elbert, S. T.; Gordon, M. S.; Jensen, J. H.; Koseki, S.; Matsunaga, N.; Nguyen, K. A.; Su, S. J.; Windus, T. L.; Dupuis, M.; Montgomery, J. A. *J. Comput. Chem.* **1993**, *14*, 1347.
- Chirlian, L. E.; Franc, M. M. *J. Comput. Chem.* **1987**, *8*, 894.